ELSEVIER

Coordination Chemistry Reviews
222 (2001) 193–218

COORDINATION CHEMISTRY REVIEWS

www.elsevier.com/locate/ccr

Giant metal-oxide-based spheres and their topology: from pentagonal building blocks to keplerates and unusual spin systems

A. Müller [a,*], P. Kögerler [a], A.W.M. Dress [b]

[a] *Faculty of Chemistry, University of Bielefeld, P.O. Box 10 0131, D-33501 Bielefeld, Germany*
[b] *Department of Mathematics, University of Bielefeld, D-33501 Bielefeld, Germany*

Received 23 October 2000; accepted 25 May 2001

Contents

Abstract

Novel synthesis strategies based on the geometrical and topological principles outlined here open up pathways to a new class of spherical clusters with icosahedral symmetry of the type $(pentagon)_{12}(linker)_{30}$—also called *keplerates*—where the centers of the 12 pentagons span an icosahedron and the centers of the 30 linkers an icosidodecahedron. Remarkably, sizing of a spherical molecule is possible for the first time. In addition to their large size of several nanometers, these molecules show unusually high symmetries. When large numbers of paramagnetic metal centers like 30 Fe^{III} or 20 VO^{2+} are integrated within their structure,

* Corresponding author. Tel.: +49-521-1066153; fax: +49-521-1066003.
E-mail address: a.mueller@uni-bielefeld.de (A. Müller).

PII: S0010-8545(01)00391-5

extraordinary spin topologies can be realized on a discrete molecular level. Further functionalization of these systems allows, e.g. to link them forming chains or layers in solid state reactions at room temperature.

Keywords: Self-assembly; Polyoxometalates; Clusters; Magnetism; Topology; Keplerates

1. Introduction

Polyoxometalate (metal-oxide-based) clusters represent a class of inorganic compounds which show an unmatched variety of molecular and electronic structures. The correspondence of their primary, very simple building units with (purely) geometric analogues formed by regular and semi-regular polyhedra such as Platonic and Archimedean solids, allows the chemist to operate conceptually with a large variety of distinct molecular modules derived from these units [1]. With the recent advent of molybdenum-oxide-based keplerates (see below) or superfullerene-type clusters, it has become possible to construct molecular spherical systems using predetermined reaction routes [2]. Different ball-shaped clusters with icosahedral symmetry are accessed easily based on versatile means of linking the fundamental pentagonal molecular fragments. These novel species, exhibiting extraordinary structural, magnetic, and electronic properties, are basically synthesized using: (1) pentagonal $\{(Mo)Mo_5\}$ building blocks (see below), also abundant in most of the larger (nanometer-sized) polyoxomolybdate clusters and (2) linker entities that interconnect these pentagons.

When it comes to characterizing the pertinent matching rules that govern the modes of the building assemblage, topological approaches turn out to be particularly helpful. These aspects are reviewed in this article together with the basic principles of the related chemistry as well as some of the resulting unprecedented magnetic features.

2. Basic chemical principles

The versatile chemistry of polyoxomolybdate clusters has resulted in an unmatched structural variety, both of discrete molecules and extended one-, two-, and three-dimensional assemblies, and provides also a number of features that offer excellent prerequisites for the synthesis of nanostructured species with well-defined structural units even under one-pot conditions. These are:

1. *Transferable building blocks*. This concept does not only refer to the geometrical/structural decomposition of polyoxometalates into entities like pentagonal bipyramids but reflects also their well-defined reactivities determining the unit-specific *local matching rules* according to which these building groups can—and will—be linked.

2. *Versatile redox chemistry*. Different degrees of reduction of the molybdenum centers of the related mixed-valence species offer the option to tune the electron density of the clusters.
3. *Integration of hetero elements and exchange of ligands*. This allows altering reactivity, functionality and the physical properties such as the magnetism of the final reaction product.
4. *Tuneable charge/size ratio*. The charge of polyoxomolybdate fragments can be modified by the exchange of special groups (e.g. $[MoNO]^{3+}$ for $[MoO]^{4+}$), by inclusion of hetero elements (see above), exchange of metal centers (e.g. V^{V} for Mo^{VI}), or by the type of reducing agent. An increased absolute (negative) charge (while keeping the charge density constant) of the intermediates in the aqueous solutions guarantees the solubility that is necessary for the ongoing molecular growth processes.
5. *Template functionality*. The formation of larger polyoxomolybdate systems is in special cases facilitated by supramolecular-type interactions between the growing fragments and other species present in the reaction solution, for instance those which can act as templates.

These principles can briefly be illustrated, e.g. by the syntheses, structures, properties, and especially the reactivities of the class of wheel-shaped tetradecameric- and hexadecameric-type clusters $\{Mo_{154}\}$ ($[Mo_{154}(NO)_{14}O_{448}H_{14}(H_2O)_{70}]^{28-}$, $[Mo_{154}O_{462}H_{14}(H_2O)_{70}]^{14-}$), which have the same type of stoichiometry as the spherical systems, i.e. $\{Mo_{11}\}_n \equiv \{(Mo)Mo_5Mo_5\}_n$ [2] and $\{Mo_{176}\}$ ($[Mo_{176}O_{528}H_{16}(H_2O)_{80}]^{16-}$) [1a,2] (final formula without error limits) [3,4]. The species consist of three types of building units: (1) The $\{Mo_8\}$-*type group* which contains a central, structurally directing pentagonal MoO_7 or $Mo(NO)O_6$ bipyramid to which five MoO_6 octahedra are adjoined sharing the five equatorial edges. This creates a pentagonal $\{(Mo)Mo_5\}$ fragment (note that the $\{(Mo)Mo_5\}$ fragment occurs also in the spherical systems [2]). Two additional MoO_6 octahedra are connected (sharing vertices) to this entity to give the characteristically curved $\{Mo_8\}$ group. (2) The $\{Mo_2\}$ *group* formed by two corner-sharing MoO_6 octahedra. (3) The $\{Mo_1\}$ *unit*. The intact $\{Mo_{154}\}$- and $\{Mo_{176}\}$-type clusters contain each of these three groups 14 and 16 times, respectively, resulting in approximate D_{7d} and D_{8d} molecular symmetry (Fig. 1). The tetra- and hexadecameric cluster systems constitute structural prototypes for the so-called molybdenum blue species [5]. They are 2×14- and 2×16-fold reduced, respectively, with the related 4d electrons trapped in 14 and 16 'compartments'. The ring systems can be derivatized, e.g. by ligand exchange reactions [6], and modified by generating defects (by the removal of the $\{Mo_1\}$ and $\{Mo_2\}$ groups which results in *lacunary* clusters showing defect positions compared with their structural archetypes and displaying enhanced reactivity, e.g. that they subsequently can condense to form chain or layer structures [7]). It is even possible to trap lacunary ring fragments and/or decrease their ring size by increasing the curvature due to the replacement of electrophilic $\{Mo_2\}$ groups by smaller ones, e.g. by electrophilic lanthanoid cations [8,9]. Under still stronger reducing reaction conditions, the $\{Mo_{176}\}$-type cluster system even starts growing again with the consequence that two (unstable)

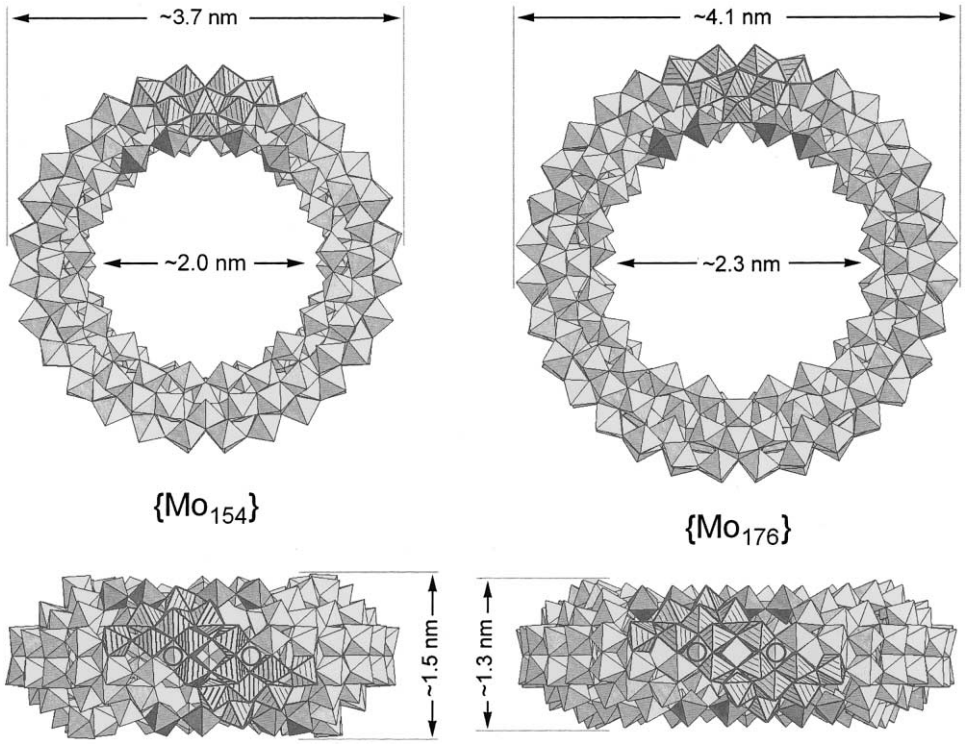

Fig. 1. Polyhedral representations of the $\{Mo_{154}\}$ (left) and the $\{Mo_{176}\}$ (right) clusters showing three different building groups (the individual polyhedra represent the MO_n coordination geometries). One $\{Mo_8\}$ group is outlined, two $\{Mo_2\}$ groups are shown in dark gray, and two equatorial $\{Mo_1\}$ units are shown encircled.

molybdenum-oxide fragments of the type $\{Mo_{36}O_{96}(H_2O)_{24}\}$ cover the cavity of the wheel-shaped cluster like hubcaps, resulting in the $\{Mo_{248}\}$-type cluster [10].

If the building-block based method of generating curved discrete molecular systems (e.g. of the ring-type) is to be extended to produce spherical systems, building blocks are needed that match both, topological and symmetry requirements. Regular pentagons are adequate for such purposes, a fact that is known since Pythagorean times. These pentagons do not tile the (Euclidean) plane, i.e. they cannot form a regular and infinitely repetitive two-dimensional pattern which is invariant with respect to two linearly independent translations. Instead, they 'agglomerate' easily in three-space forming a closed three-dimensional solid, the *dodecahedron* (Fig. 2). Thus, the pentagonal $\{(Mo)Mo_5\}$ group with its C_5 symmetry that is present in the $\{Mo_8\}$ group of the giant wheel-type species (Fig. 4), can also be utilized as a potential building block for constructing spherical clusters of icosahedral symmetry. This icosahedral symmetry (C_5 C_3 C_2) can be obtained even if the pentagons do not share edges, but are interconnected by appropriate linkers (Fig. 3). In the aqueous reaction solution, at appropriate pH value, and in the

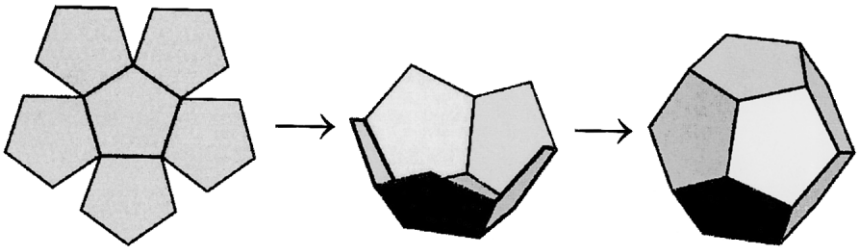

Fig. 2. Regular pentagons cannot be densely packed to form a two-dimensional array with translational symmetry (left) but when folded up can form a closed polyhedron, i.e. the dodecahedron (right).

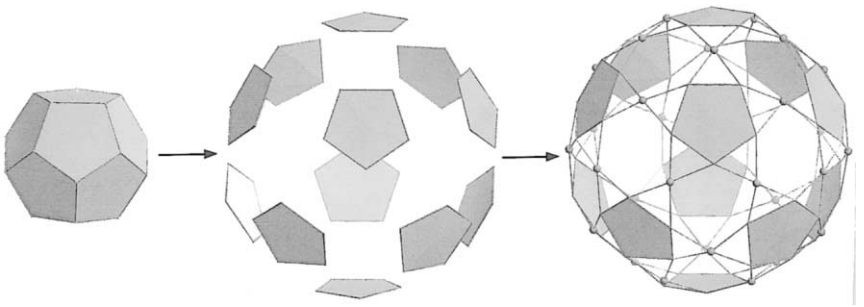

Fig. 3. Schematic transition from a dodecahedron (left) via an 'extended' polyhedron based on 12 separated pentagons which are finally interconnected by linker units (small spheres) to form a larger spherical system while the I_h symmetry is retained in both steps.

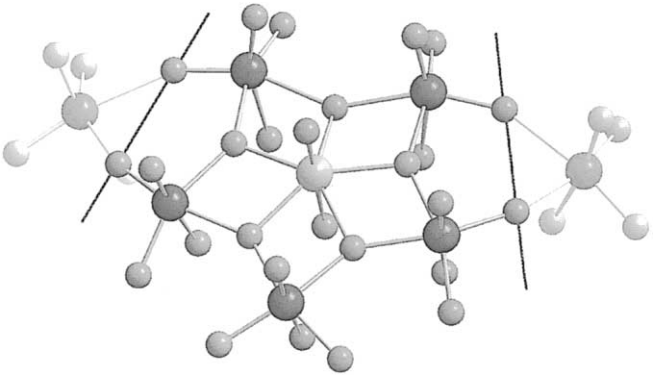

Fig. 4. Structure of the $\{Mo_8\}$ building group of the giant wheel-type cluster in ball-and-stick representation. One part, the $\{(Mo)Mo_5\} \equiv [(Mo)Mo_5O_{21}]^{6-}$ fragment, i.e. the basic building block of the spherical clusters, is emphasized: the two gray lines illustrate the separation of the $\{(Mo)Mo_5\}$ entity from the two adjoined MoO_6 octahedra. Mo: dark gray (central Mo: bright gray), O: gray.

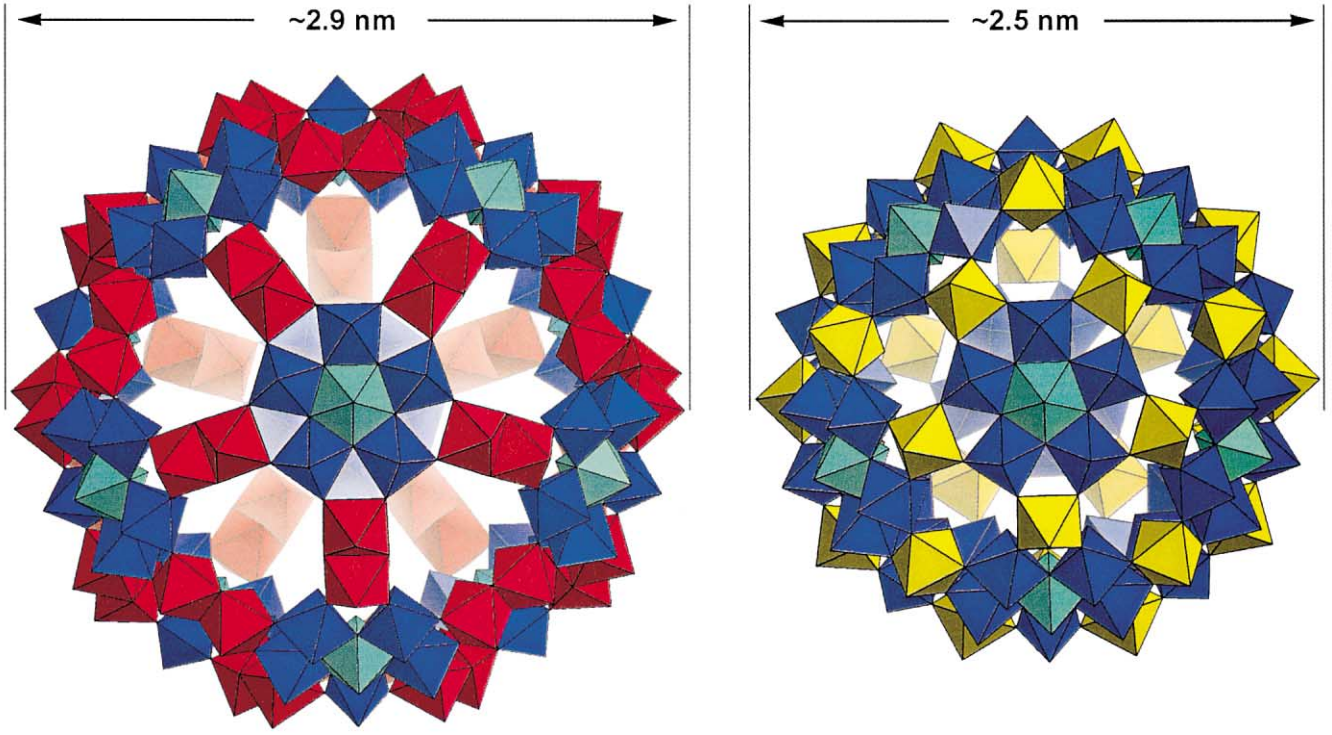

Fig. 5. Structural comparison of the $\{Mo_{132-}\}$- (left) and $\{Mo_{72}Fe_{30}\}$-type (right) clusters. Both consist of 12 $\{(Mo)Mo_5\}$ groups (blue, with the pentagonal MoO_7 bipyramids in bright blue). The different linker groups L ($\{Mo_{132}\}$:L = $\{Mo_2^V\}$, red; $\{Mo_{72}Fe_{30}\}$: L = $\{Fe\}$, yellow) can be used for a novel type of sizing.

presence of (small) linkers each of which can interconnect two of the pentagonal units, the $\{(Mo)Mo_5\}$ units basically self-assemble to form a molecular icosahedral species containing 12 of these C_5-type pentagons and 30 linkers. Each linker shares vertices with each of the two $\{(Mo)Mo_5\}$ groups it joins. Suitable for this type of linking are, for instance, dinuclear dumb-bell shaped $\{Mo_2^V\}$ groups (stabilized by a bidentate ligand, e.g. an acetate anion in $[Mo_2^VO_4(CH_3COO)]^+$) [11] or mononuclear fragments like $[Fe^{III}(OH_2)_2]^{3+}$ [12] and $[OMo^V(OH_2)]^{3+}$ [13].

Relevant cluster species are $[\{(Mo)Mo_5O_{21}(H_2O)_6\}_{12}\{Mo_2^VO_4(CH_3COOH)\}_{30}]^{42-}$ ($\{Mo_{132}\}$, present in the compound $(NH_4)_{42}\{Mo_{132}\}\cdot ca.\ 300H_2O\cdot ca.\ 10CH_3COONH_4$), and the neutral mixed-valence cluster $[\{(Mo)Mo_5O_{21}(H_2O)_4(CH_3COO)\}_{12}\{MoO(H_2O)\}_{30}]$ ($\{Mo_{102}\}$, found in $\{Mo_{102}\}\cdot 150H_2O$) (Fig. 5). The latter cluster is an analog of the $\{Mo_{72}Fe_{30}\}$ cluster containing also 102 metal atoms. All these species are of the $(pentagon)_{12}(linker)_{30}$ type.

In all the spherical systems, the centers of the 12 pentagonal $\{(Mo)Mo_5\}$ units are positioned at the vertices of an icosahedron. While the special linkers $[Mo_2^VO_4]^{2+}$ in the $\{Mo_{132}\}$-type cluster define the 90 edges of a distorted (non-regular) truncated icosahedron with 20 hexagons (with C_3 symmetry) and 12 pentagons comparable approximately to the C_{60} fullerene (Fig. 6), the centers of the 30 linker units form an icosidodecahedron, consisting of 12 pentagons and 30 triangles (Fig. 7). In these two Archimedean solids, the $\{(Mo)Mo_5\}$ pentagons are either 'condensed' (e.g.

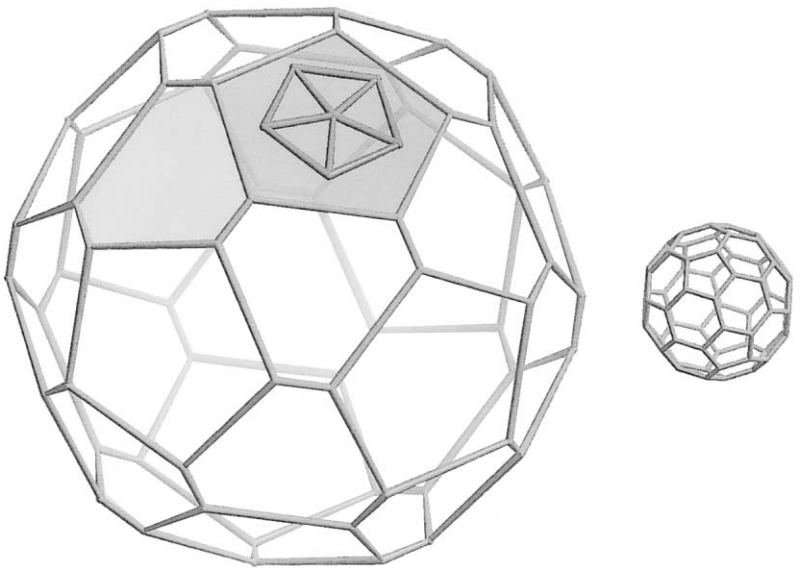

Fig. 6. Structure of the icosahedral $\{Mo_2^V\}_{30}$ fragment of the $\{Mo_{132}\}$ cluster with 12 regular pentagons and 20 hexagons showing trigonal symmetry as well as its coherence to the C_{60} fullerene, which is depicted on the same scale. The metal skeleton of a single $\{(Mo)Mo_5\}$ pentagon occurring in all clusters discussed here is shown in its actual position.

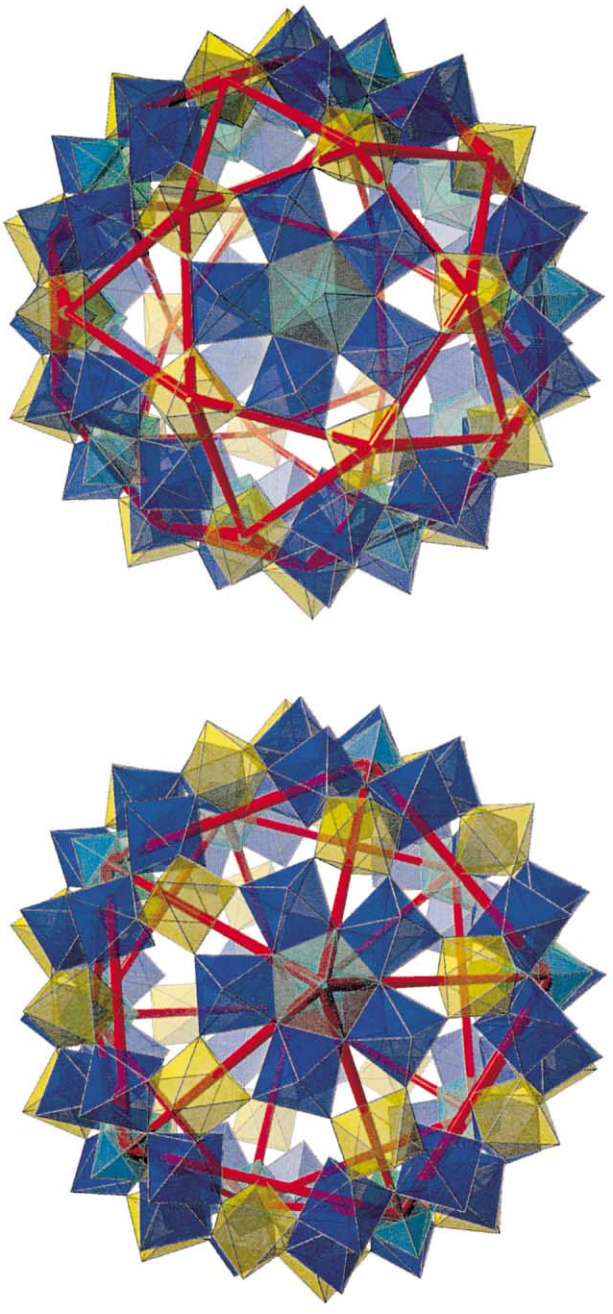

Fig. 7. Transparent polyhedral representation of the $\{Mo_{72}Fe_{30}\}$-type keplerate with the inscribed polyhedra (red), i.e. the icosahedron (defined by the 12 central positions of the $\{(Mo)Mo_5\}$ groups, left) and the icosidodecahedron (formed by the 30 Fe centers, right). See Fig. 5 for color code.

when linked by the mononuclear linkers Fe^{III} or Mo^{V}) or 'isolated' as in the large $\{Mo_{132}\}$ cluster that may be dubbed an inorganic superfullerene. In the resulting spherical geometry of all these clusters, the local fivefold symmetry of the $\{(Mo)Mo_5\}$ groups is retained. In addition, the icosahedral systems also show 15 twofold symmetry axes crossing the centers of the linkers and 10 threefold axes crossing the barycenter of three neighboring pentagonal units.

It is of particular interest that—by virtue of Euler's theorem—exactly 12 pentagonal units are essential for the optimal construction of spherical polyhedral structures (pseudoicosahedra): Pentagons are present in the 'magic number' of 12—along with a defined number of hexagons—in such types of formations like viruses, small organisms (e.g. in Haeckel's celebrated radiolaria [14]), and even in the largest known spherical polyhedral objects such as Buckminster Fuller's geodesic structures, for instance that one housing the US Expo '67 exhibit in Montreal.

In view of Kepler's fascination by and early insights into pentagonal symmetry as demonstrated by his famous model of the cosmos, it has been suggested to call every spherical species of icosahedral symmetry a *keplerate*. Kepler depicted his visionary model of planetary motion in his speculative work *Mysterium Cosmographicum* [15] according to which the radii of successive planetary orbits are proportional to the radii of spheres that are successively circumscribed around and inscribed within the five Platonic solids. This situation is reflected in the present molecular systems.

In the case of the $[\{(Mo)Mo_5O_{21}(H_2O)_6\}_{12}\{Mo_2^{V}O_4(CH_3COOH)\}_{30}]^{42-}$ cluster, the icosahedron formed by the central atoms of the 12 $\{(Mo)Mo_5\}$ groups is circumscribed by a spherical shell spanned by the remaining metal atoms. Yet, as we will see in the next section, such complex geometric shapes are to be expected when dealing with keplerates.

3. Topology of the keplerate clusters and magic numbers of spherical objects

As mentioned already, the $\{Mo_2^{V}\}_{30}$ fragment within the $\{Mo_{132}\}$ cluster shows striking similarities with the famous C_{60} fullerene (Fig. 6). Remarkably, its topology is also reminiscent of that of certain spherical viruses ([11a], see also Fig. 8).

These spherical viruses display 60 copies of an identically packed fundamental structural motif whose constituents can formally be grouped into pentagonal and hexagonal *capsomers* (morphological units of chemically identifiable oligomers consisting of one or more viral proteins or protein subunits). One of the simplest examples is the satellite tobacco necrosis virus (STNV) in which only 12 pentagonal capsomers with a total of 60 identical viral protein subunits—coded by one gene only—are placed at the 12 vertices of an icosahedron (Fig. 8). In larger spherical viruses—for example those with $3 \times 60 = 180$ subunits—the motif that occurs 60 times contains three protein monomers, one that is part of a pentagonal capsomer and two that are part of a hexagonal capsomer. In other words, viewing the virus as being organized in capsomers, there are 12 pentagonal capsomers each consisting

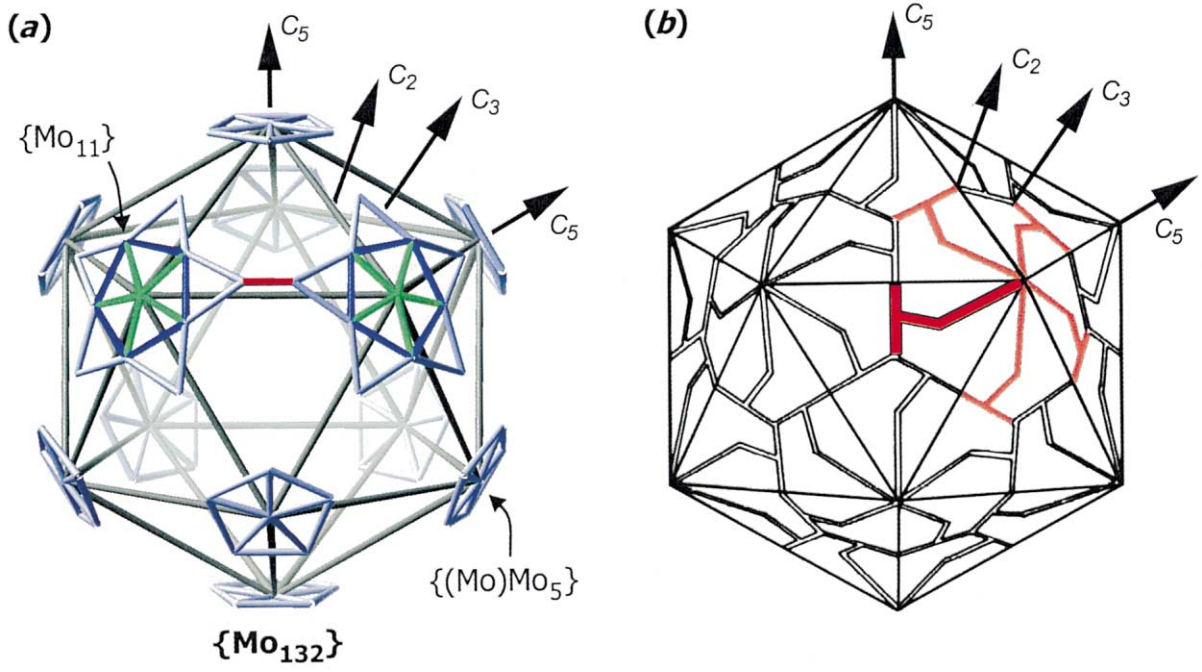

Fig. 8. Schematic representation of the icosahedron spanned by the centers of the $\{(Mo)Mo_5\}$ subfragments of the $\{Mo_{132}\}$-type cluster (a) and of the satellite tobacco necrosis virus (STNV) with triangulation number $T = 1$ (for further details see Ref. [11]) highlighting five of the protomers (red) (b). In the case of the $\{Mo_{132}\}$ cluster two $\{Mo_{11}\}$ units (see Ref. [2] for this building group) each formed by the $\{(Mo)Mo_5\}$ groups, and the five related Mo centers of the five neighboring $[Mo_2^{V}O_4]^{2+}$ linkers are emphasized.

of five identically connected protein monomers centered at the vertices of an icosahedron, and 20 additional hexagonal capsomers each one built up from six protein monomers (note that 60×3 equals $12 \times 5 + 20 \times 6$).

According to Goldberg [16] and, independently, to Caspar and Klug [17] who were inspired by Fuller's geodesic domes, such structures can be constructed from gluing together 20 identical copies of an (arbitrarily large) equilateral *parent* triangle cut out appropriately from the standard 'Platonic' tiling of the plane by congruent (small) *basic* equilateral triangles (see Fig. 9, for further details and references see Ref. [18]).

Note in particular that the parent triangles are parameterized easily by a pair (h, k) of integers with $h > 0$ and $k \geq 0$ and that—using this parameterization—their area is $T = T(h, k) := h^2 + hk + k^2$ times larger than that of the basic ones. The resulting solids are called icosadeltahedra. In general, their subunits exhibit, in addition to the global symmetry inherited from the *parent icosahedron*, also some local sixfold (quasi-) symmetry.

Clearly, the icosahedron itself as well as the capped icosahedron are such solids. More generally, as was shown as early as 1937 by Goldberg, a solid is an icosadeltahedron if and only if it has icosahedral symmetry and its faces are exclusively triangles, with either exactly five or six of them meeting at each of the polyhedron's vertices.

It follows in particular that the number of capsomers in an icosahedral virus with triangulation number T—and, hence, consisting of $60T$ protein monomers—is $2 + 10T$, the so-called *magic number* associated with T, because—quite generally—$5 \times 12 = 60$ of those protein monomers form the topologically required 12 pentagonal capsomers while the remaining $60T - 60 = 60(T - 1)$ form $60(T - 1)/6 = 10(T - 1)$ hexagonal capsomers, giving rise to altogether $12 + 10(T - 1) = 2 + 10T$ capsomers (for further details, see Coxeter [19], Goldberg [16], and Stewart [20]).

Consequently, the larger—and more abundant—spherical viruses such as the tomato bushy stunt virus (TBSV) can easily consist of more than 60 protein

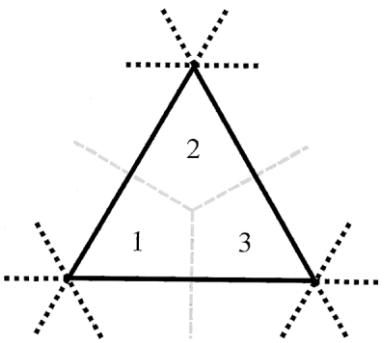

Fig. 9. Three fundamental subunits in a basic triangle. The subunits form the intersection of the basic triangles and the hexagons of the dual hexagonal tiling.

monomers. A viral structure with $T=3$ ($h=k=1$) consists of 180 ($=3\times 60$) protein monomers forming 32 capsomers whereas the triangulation number $T=1$ ($h=1,\ k=0$) applies to the small (10 nm) STNV mentioned above. This also applies to that fragment in each of the three polyoxomolybdate clusters discussed above which consists of the 60 MoO_6 octahedral subunits altogether (of which five at a time, together with the 12 central pentagonal bipyramids MoO_7, form the 12 $\{(Mo)Mo_5\}$ pentagonal building blocks). For the above-mentioned Buckminster Fuller's topologically comparable geodesic dome, we have $T=36$ ($h=6,\ k=0$).

Note, by the way, that the parameters h and k are, in general, not determined by their triangulation number $T=T(h,k)=h^2+hk+k^2$, and that $T(h,k)=T(h',k')$ can hold for rather distinct parameter values h, k and h', k'. Indeed, we have $T(1,11)=133=T(9,4)$ (see Ref. [18] for more details).

In the present context of highly symmetric polyhedral objects of roughly spherical shape, it is worthwhile to extend the class of molecular species that should be designated to represent a keplerate to encompass just any (inorganic) molecular species with (proper or full) icosahedral, octahedral, or tetrahedral symmetry. More specifically, such molecular species might also be designated to represent *icosahedral*, *octahedral*, and *tetrahedral* keplerates. Clearly, every keplerate has, essentially by definition, one central point, its *barycenter*—whether or not occupied by an atom—and its atoms are organized in one or more spherical shells around this central point while each symmetry class of atoms forms the set of vertices of a Platonic or a (generalized) Archimedean solid.[1]

Extending this definition further, we may define any convex polyhedron in three-space with full or proper icosahedral, octahedral, or tetrahedral symmetry to be a keplerate or—more precisely—an I_h, O_h, or T_h (or I, O, or T) keplerate, respectively.

Clearly, given a keplerate P with symmetry group Σ ($=I_h$, O_h, T_h, I, O, or T) to begin with, we may classify the points v in $\mathbf{E}^3$ relative to Σ according to (the type of) their local, or point symmetry subgroup, i.e. the *stabilizer* subgroup

$$\Sigma_v := \{\sigma\in\Sigma \,|\, \sigma(v)=v\}$$

of v in Σ consisting of all symmetries σ in the full symmetry groups Σ that fix the point v. Recall that the *order* (or cardinality) of the *symmetry class* $\{\sigma(v)|\sigma\in\Sigma\}$ of a point v in $\mathbf{E}^3$ always coincides with the *index* of its stabilizer subgroup in Σ (i.e. with the integer one gets by dividing the cardinality or order of Σ by the order of its point symmetry group Σ_v, which is always a divisor of the former according to Lagrange's theorem).

[1] Essentially by definition, a Platonic solid is a convex polyhedron whose symmetry group acts transitively on its set of vertices, edges, and faces, while an Archimedean solid is a convex polyhedron whose symmetry group acts transitively just on its set of vertices and whose edges all have the same length. Dropping the latter requirement, we arrive at the class of generalized Archimedean solids. It is easy to see, yet still remarkable, that topologically—that is, apart from measure and proportion (cf. Ref. [21])—there is no difference between Archimedean solids and generalized Archimedean solids: the various edges in a generalized Archimedean solid can always be rescaled so that a proper Archimedean solid results.

Clearly, there is exactly one point $v = v_\Sigma$—the center of gravity of P—whose stabilizer group is the full symmetry group Σ. In any coordinate system used to specify Σ and/or P, this point is generally taken to be the coordinate system's origin, and we will therefore refer to it below as the *coordinate center*.

In view of the importance of icosahedral structures within the general context referred to above as well as within the context of polyoxometalate chemistry in particular (and also to suppress unnecessary technicalities), we will restrict our attention in the following, exclusively to structures with proper icosahedral symmetry, i.e. to I keplerates.

In this case, the stabilizer group Σ_v of any point v in $\mathbf{E}^3$ that is distinct from v_Σ, is either the trivial group C_1, or it is one of the groups C_2, C_3, or C_5, that is, it is a cyclic group consisting of (the identity transformation and) one twofold, two threefold, or four fivefold rotations around a fixed axis connecting v with the coordinate center.

Moreover, the special structure of the icosahedral symmetry group implies that all points v in $\mathbf{E}^3$ with a given fixed distance to the coordinate center and local symmetry group of type either C_2, C_3, or C_5 are in the same symmetry class. Consequently, our assumption that keplerates are, by definition, supposed to be convex polyhedra (and, hence, cannot contain two distinct vertices on the same ray originating from the coordinate center) implies that the set of vertices in an I keplerate contains at most one symmetry class of order $30 = 60/2$, at most one of order $20 = 60/3$, and at most one of order $12 = 60/5$ while all other orbits must have order 60. Note, however, that this does not hold anymore for non-convex structures: In each of the three clusters $\{Mo_{132}\}$, $\{Mo_{102}\}$, and $\{Mo_{72}Fe_{30}\}$, the two oxygen atoms at the tips of each of the 12 pentagonal bipyramids MoO_7 as well as the corresponding central Mo atoms themselves, all lie on the same fivefold symmetry axis and, together, form three distinct symmetry classes of order 12.

It follows already from this simple observation that the total number N of atoms in an I keplerate (or the number of equivalent atoms in a fully symmetric fragment) cannot be arbitrary. Instead, it is necessarily one of the following eight forms:

$N = 60n$. All atoms have trivial local symmetry; examples for $n = 1$ are provided by the Mo_{60} fragments spanned by the $60 = 12 \times 5$ Mo atoms within the MoO_6 octahedra in all three clusters discussed above and, for $n = 2$, by the collection of all 120 Mo atoms in the Mo_{132} cluster outside the centers of the 12 pentagonal units.

$N = 12 + 60n$. Atoms with trivial and fivefold symmetry, only; examples for $n = 1$ are provided by the collection of all 72Mo atoms in the 12 $\{(Mo)Mo_5\}$ units in each of the three clusters and, for $n = 2$, by all 132 Mo atoms in the $\{Mo_{132}\}$ cluster.

$N = 20 + 60n$. Atoms with trivial and threefold symmetry, only.

$N = 30 + 60n$. Atoms with trivial and twofold symmetry, only; examples for $n = 0$ are the 30 Fe atoms of $\{Mo_{72}Fe_{30}\}$ and the 30 Mo atoms within $\{Mo_{102}\}$.

$N = 32 + 60n$. Atoms with trivial, threefold and fivefold symmetry, only.

$N = 42 + 60n$. Atoms with trivial, twofold and fivefold symmetry, only; examples for $n = 1$ are provided by all metal atoms in the $\{Mo_{72}Fe_{30}\}$ cluster as well as in

the $\{Mo_{102}\}$ cluster; an example for $n = 0$ is provided by $\{Mo_{72}Fe_{30}\}$ with the 30 Fe atoms together with the 12 Mo atoms that are the centers of the 12 pentagonal subunits spanning an icosahedron.

$N = 50 + 60n$. Atoms with trivial, twofold and threefold symmetry, only.

$N = 62 + 60n$. Atoms with all types of local symmetry.

Here, n is any non-negative integer, and one has $n = 0$ if and only if every atom has a non-trivial local symmetry. Note that, for a given n, there can be one or more

Table 1
Combinatorial types of I keplerates

N	I keplerates	I_h keplerates	I tilings	I_h tilings	Non-polyhedra 1 I tilings	Non-polyhedral I_h tilings
12	1	1	1	1		
20	1	1	1	1		
30	1	1	1	1		
32	3	3	3	3		
42	1	1	1	1		
50	1	1	1	1		
60	4	3	4	3		
62	3	3	3	3		
72	9	7	11	9	2	2
80	9	7	11	9	2	2
90	7	7	7	7		
92	28	23	32	27	4	4
102	16	15	18	17	2	2
110	16	15	18	17	2	2
120	44	23	50	27	6	4
122	39	31	43	35	4	4
132	123	71	161	101	38	30
140	123	71	161	101	38	30
150	89	67	99	75	10	8
152	368	207	467	285	99	78
162	214	139	263	175	49	36
170	214	139	263	175	49	36
180	656	223	824	311	168	88
Total	1970	1059	2443	1385	473	326

For any given number N of atoms up to $N = 180$, this table lists the number of combinatorially (or, equivalently, *topologically*) distinct I and I_h keplerates as well as the (larger) number of combinatorially distinct tilings of the sphere with I and I_h symmetry, respectively, and—finally—the differences between corresponding pairs of numbers, i.e. the number of such tilings that are not combinatorially equivalent to (and, hence, cannot be derived from) a corresponding keplerate. The algorithms used for computing the numbers in this table actually do not only compute the numbers given, but also yield the Delaney symbol of each tiling. They are based on the methods developed in Ref. [23]. Remarkably, the numbers that result for $N = 12+30c+60n$ and $N = 20+30c+60n$ (c either $= 0$ or 1, n any natural number) always coincide. For icosahedral tilings, this is a simple consequence of the theory of Delaney symbols [23] or—almost equivalently—the theory of orbifolds [24]. For the keplerates, some additional reasoning is necessary based on Ernst Steinitz' classical theorem (and its more recent elaboration by Peter Mani) that an (equivariant) spherical tiling is (equivariantly) *realizable* as a polyhedron if and only if it is three-connected.

distinct 'combinatorial' types of I keplerates (see Table 1). For $n = 0$, there is—up to equivalence—exactly one I keplerate with 12, 20, or 30 atoms, respectively, the icosahedron, the dodecahedron, and the icosidodecahedron, all actually having full icosahedral symmetry I_h, while there are four distinct types of I keplerates with 60 atoms, all but one having realizations with full icosahedral symmetry. There is also exactly one keplerate with 50 and exactly one keplerate with 42 atoms, while there are three types of keplerates with 32 atoms and three types with exactly 62 atoms, all eight types also exhibiting full icosahedral symmetry.

Clearly, every I keplerate gives rise to an *icosahedral tiling*, that is a tiling of the sphere with icosahedral symmetry: One can project the straight edges of any convex I keplerate from the coordinate center onto any sphere with the same center surrounding the keplerate. It is worth noting that not all tilings of the sphere with I symmetry arise in this way. For example, there are two tilings with exactly 72 and two with exactly 80 atoms that cannot be derived in this manner. However, combinatorial methods permit one actually to enumerate all such spherical tilings even though combinatorial explosion sets in rapidly: There are seven such tilings with 90 vertices, 50 with 120 vertices, and there are altogether 23 691 tilings of the sphere with I symmetry with at most four distinct symmetry classes of vertices of which 16 328 are necessarily chiral while the remaining 7363 tilings can be realized so that they exhibit full icosahedral symmetry.

This implies that, without further restrictions, classification and enumeration—though mathematically possible—does not give much further insight.

However, there is a way that allows one to proceed much beyond icosahedral structures with, say, four or five distinct symmetry classes of vertices/atoms by restricting attention to operations that construct (complex) keplerates from (simple) keplerates which we will now discuss.

Above, we have discussed Goldberg's procedure that allowed us to construct icosideltahedra from the planar tiling built up exclusively from congruent equilateral triangles. Remarkably, this procedure can be generalized as well as inverted quite easily:

Given a tiling T of the sphere with icosahedral symmetry (or, for short, an icosahedral tiling), we can always assume that it is realized not on the sphere, but on the icosahedron such that its symmetry group is exactly the symmetry group of that icosahedron. This is true even for structures like, say, the dodecahedron which can be realized by choosing the midpoints of the various equilateral triangles of the icosahedron as the dodecahedral vertices and by connecting them by broken lines that stretch from those midpoints of the icosahedral triangles first straight to the midpoints of their respective edges and then straight on to the midpoint of the adjacent triangle (see Fig. 10).

We can now cut out one of the resulting 20 equilateral triangles of the icosahedron, take infinitely many copies of it, and place them in a regular fashion into the Euclidean plane, always six around each vertex. By applying this for the dodecahedral tiling of the icosahedron described above, the regular hexagonal tiling of the Euclidean plane will thus be created. In any case, this method will always produce a tiling T' of the Euclidean plane with infinitely many symmetry-equivalent centers of sixfold rotational symmetries.

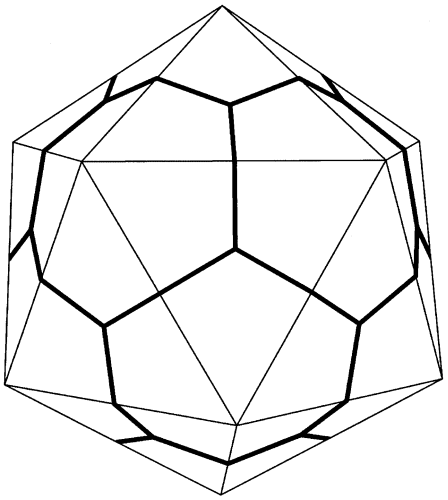

Fig. 10. The dodecahedral tiling realized by implanting 20 triangles into the icosahedron cut out from the planar hexagonal tiling as described in the text.

Thus, we can now apply Goldberg's procedure by choosing an arbitrary equilateral parent triangle all of whose vertices are centers of sixfold rotational symmetry, and construct a new tiling T'' of the icosahedron (with icosahedral symmetry) by gluing together 20 copies of this large triangle as described above.

If we apply this construction to the icosahedron itself, we will get exactly the family of icosadeltahedra; if we apply it to the dodecahedron, we get exactly the family of fullerene structures with icosahedral symmetry (see Ref. [22]).

Clearly, there are many further options for defining operators of this kind all of which can most easily be defined by: (a) referring to the theory of *Delaney symbols* (cf. Ref. [23]) and *orbifolds* (cf. Ref. [24]) and (b) combining this theory with methods for determining specific subgroups of crystallographic groups as studied in *symmetry breaking*, see, for instance, Ref. [25].

4. The magnetism of spherical polyoxometalates

The ability to generate polyoxometalate systems with high numbers of unpaired electrons has yielded a variety of clusters with extraordinary magnetic properties [1b,26]. Magnetic molecular clusters are currently investigated in great detail [27], e.g. in order to study quantum size effects in magnets [28]. In fact some molecular clusters have been termed single-molecule magnets [29] in order to stress with a somewhat emphatic designation their unique properties. Polyoxometalates have been shown to give rise to a behavior reminiscent of that of magnetic multilayers [30] but there are difficulties in observing real bulk behavior in clusters containing $s = 1/2$ magnetic centers, because the spin carriers have an intrinsically quantum

nature. Therefore very large numbers of metal ions must be assembled in order to observe complex magnetic behavior.

The recent synthesis of giant polyoxometalate cluster systems has indeed allowed us to incorporate the required high number of paramagnetic functions and to (approximately) arrange them on a spherical surface. Referring to such molecular magnets based on polyoxomolybdates, paramagnetic centers can be embedded in a structure-determining diamagnetic polyoxomolybdate framework to form a magnetic polyhedron (such as the Fe_{30} icosidodecahedron in $\{Mo_{72}Fe_{30}\}$) exhibiting intriguing magnetic properties which are intermediate between simple molecular paramagnetism and bulk magnetism (for general discussions see Ref. [31]). From a functional point of view, the resulting clusters can be viewed as composed of: (1) a basically diamagnetic polyoxomolybdate framework (e.g. based on $\{(Mo)Mo_5\}$ groups) and (2) a framework of paramagnetic centers—such as V^{IV}, Fe^{II} or Fe^{III}—with unusual spin topology connecting the diamagnetic pentagonal polyoxomolybdate fragments. These discrete molecular systems show very weak intermolecular and comparatively strong intramolecular interactions.

Polyoxomolybdate fragments can act as particularly efficient transmitters of magnetic exchange, i.e. as strong superexchange ligands. In $\{Mo_{57}M_6\}$-type cluster systems, for example, it is possible to place different (para-)magnetic centers M like $Fe^{II/III}$ and $V^{IV}O^{2+}$ at the respective linker positions to form a trigonal M_6 prism with intramolecular distances larger than 0.6 nm [32]. The magnetism of these systems with special linkers shows strong antiferromagnetic or ferrimagnetic interactions, depending also on the protonation and the reduction state of the polyoxomolybdate framework. In addition, the cluster's magnetic properties can also be controlled—or even tuned—by stepwise exchange of individual magnetic centers [33].

4.1. A keplerate with 30 high-spin-iron(III) centers

The reaction of Fe^{III} ions in aqueous media with polyoxomolybdate solutions of appropriate pH value in which $\{(Mo)Mo_5\}$ groups exist as virtual units, results in the formation of a water-soluble icosahedral $\{Mo_{72}Fe_{30}\}$-type cluster (see above). The 30 Fe^{III} ($s = 5/2$) centers are bound to two oxygen atoms of two MoO_6 octahedra belonging to two $\{(Mo)Mo_5\}$ groups, resulting in a (slightly distorted) octahedral $[Fe^{III}O_{eq,4}(OH_2)_{ax,2}]$ group. Despite their relatively wide spacing (0.64 nm), the Fe centers which define the sites of a regular icosidodecahedron, show a significant antiferromagnetic interaction [12,34]. This yields the $\{Mo_{72}Fe_{30}\}$ keplerate, a molecular paramagnet with the highest number of spin centers to date. At high temperatures ($T = 300$ K), the magnetic moment of the $\{Mo_{72}Fe_{30}\}$ cluster nearly equals that of a molecular spin-only system consisting of 30 uncorrelated $s = 5/2$ centers. Down to low temperatures (about 20 K), the temperature dependence of the molar susceptibility is very well described by a Curie–Weiss term $\chi = C/(T - \Theta)$ with $C = 128$ emu K mol^{-1} (according to 30 $s = 5/2$ centers with $g = 1.974$) and $\Theta = -21.6$ K. Interestingly, the susceptibility deviates from the simple Curie–Weiss law at the lowest temperatures, passing through a weak

maximum at ca. 1.7 K and finally approaching a constant value of 6.65 emu mol^{-1} at 0.12 K.

It turned out that, due to the high s values of the individual Fe^{III} centers, the magnetism of this keplerate can be described using a classic Heisenberg model even down to temperatures as low as 0.12 K [34]. In this model, nearest neighbor spin interactions involve only a single isotropic exchange constant. Simulations based on this classical Heisenberg model indeed reproduce well all susceptibility features observed experimentally (at very low temperatures, it is necessary to apply a correction for displaced Fe^{3+} impurities by including a Brillouin term). It can be deduced from these simulations as well as from a graph theory analysis [35] that, in a magnetic icosidodecahedron, the spins exhibit geometrical frustration (at low temperatures), with all 30 spin vectors being coplanar and oriented in a regular, yet *non*-antiparallel manner. The ordering of the 30 spins at very low temperatures can be described in terms of three sublattices each of 10 spins. In these sublattices the angle between a given spin and each of its four nearest neighbors equates 120°. This ordering results in a rigorous low-temperature limit of $\chi = 4.67$ emu mol^{-1} which corresponds very well to the value determined experimentally when corrected for paramagnetic impurities.

In contrast, the spin vectors forming a regular octahedron are (at 0 K) coplanar and align with an angle of 120°. In the case of a spin dodecahedron and a spin icosahedron the vectors are found to organize in a non-coplanar manner with spin–spin angles of 138.2 and 117.6°, respectively [34].

In the $\{Mo_{72}Fe_{30}\}$ system, quantum effects are expected to be observed only below 0.05 K, as a simplified quantum model indicates [36]. Thus, the $\{Mo_{72}Fe_{30}\}$ keplerate can be regarded as the first mesoscopic magnetic molecule, which complies with a classical model even down to temperature regions typical for the quantum regime.

In a solid state reaction at room temperature, the $\{Mo_{72}Fe_{30}\}$ keplerate can be condensed further (while some of its crystal water molecules are lost) to form layer structures in which every $\{Mo_{72}Fe_{30}\}$ entity is linked to four nearest neighboring entities via linear Fe–O–Fe bridges [37]. Here, the χT value at 300 K decreases to 113 emu K mol^{-1} which compares to 113.75 emu K mol^{-1} for $30 - 4 = 26$ uncorrelated $s = 5/2$ centers. This is due to the fact that the iron centers of linear Fe–O–Fe groups are strongly antiferromagnetically coupled and contribute only negligibly to the overall magnetic moment (Fig. 11) (see also Ref. [38]).

4.2. A {$Mo_{75}V_{20}$}-type cluster containing 20 vanadium(IV) centers

$\{(Mo)Mo_5\}$ pentagons can also be used in the presence of other building blocks to construct derivatives of the afore-mentioned $\{Mo_{72}Fe_{30}\}$-type cluster which has 12 of these pentagonal $\{(Mo)Mo_5\}$ units: this can, for instance, lead to the cluster anion $[\{(Mo)Mo_5O_{21}(H_2O)_3\}_{10}\{NaSO_4\}_{10}\{V^{IV}O(H_2O)\}_{20}\{Mo^{VI}O_3(H_2O)\}_{10}\{Mo^{VI}O_2(H_2O)_2\}_5]^{20-}$ ($\equiv \{Mo_{75}V_{20}\}$) [39] which can be referenced to one of the Archimedean solids, namely the icosidodecahedron with 30 vertices and 32 faces

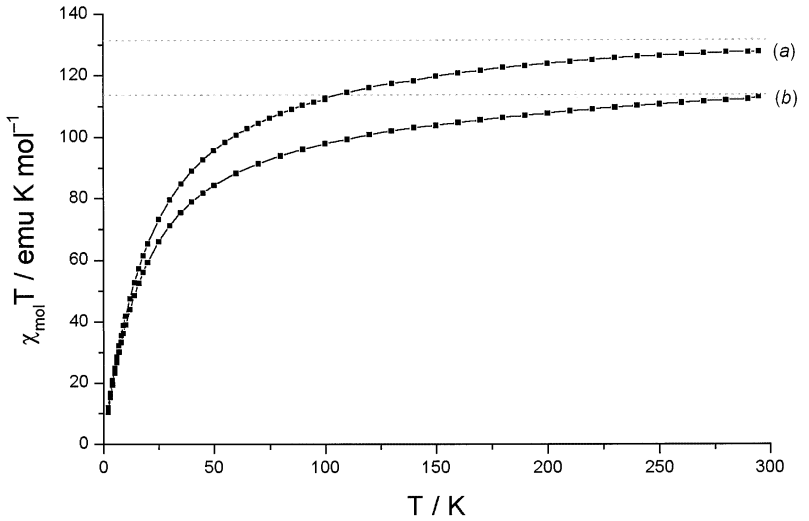

Fig. 11. $\chi_{mol}T$ vs. T graphs of the (discrete) $\{Mo_{72}Fe_{30}\}$ keplerate (a) and the corresponding layer compound $[H_4Mo_{72}Fe_{30}O_{254}(CH_3COO)_{10}\{Mo_2O_7(H_2O)\}\{H_2Mo_2O_8(H_2O)\}_3(H_2O)_{87}]\cdot$ ca. $80H_2O$ (b). The gray horizontal lines indicate the spin-only limits for 30 (upper line) and 26 (lower line) uncorrelated $s = 5/2$ centers.

(Fig. 12), which is formed by 12 pentagonal and 20 triangular faces (ten $\{V_3\}$ (see below) and ten $\{VMo_2\}$ triangles) built up by 20 V^{IV} and 10 Mo^{VI} centers. While ten of the 12 pentagonal faces of the icosidodecahedron are formed by one Mo^{VI} and four V^{IV} centers and are capped by $\{(Mo)Mo_5\}$ pentagons, the two remaining pentagonal faces are both spanned by five Mo^{VI} centers (top and bottom, lying perpendicular to the principal C_5 axis of the cluster). They are capped by one (under-occupied) array formed by five MoO_6 octahedra. In contrast to the $\{(Mo)Mo_5\}$ units, the central pentagonal bipyramidally coordinated Mo^{VI} center is missing in these $\{Mo\}_5$ arrays. Interestingly, the 20 V^{IV} centers form a ring of ten linked triangles (V–V: 6.27–6.46 Å) coordinated to four bridging oxygen atoms, thus forming two groups: (i) ten equatorial V^{IV} centers showing outward-projecting H_2O ligands and *trans*-terminal oxygen and (ii) the ten remaining V^{IV} centers exhibiting outward-projecting terminal oxygen and *trans*-terminal H_2O ligands. This results in a novel equatorial paramagnetic ring-shaped band with very strong antiferromagnetic exchange interactions. In analogy to the $\{Mo_{57}M_6\}$ systems, we believe that the 20 $V^{IV}O^{2+}$ groups should be replaceable by Fe^{III} centers.

With regard to the theory of magnetism, the $\{Mo_{75}V_{20}\}$ cluster is interesting in view of its ring of ten V^{IV} (d^1) triangles, each sharing two vertices with each of its two neighboring triangles as shown in Fig. 13. In the case of antiferromagnetic coupling, the resulting spin topology gives rise to strong frustration effects [40]. Spin frustration is currently of interest because it gives rise to highly degenerate ground states which in turn cause such spin systems to display unusual magnetic

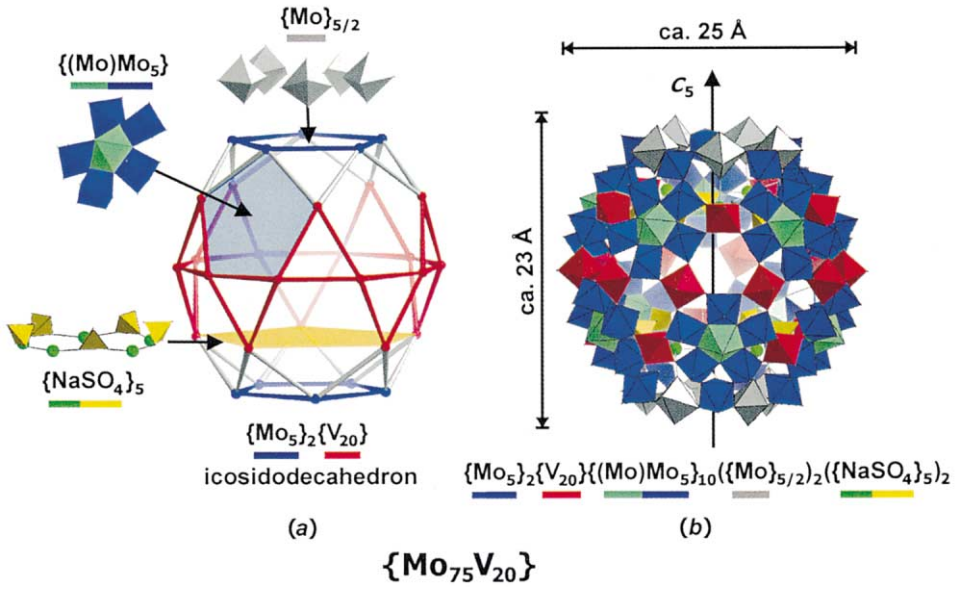

Fig. 12. Structure of the $\{Mo_{75}V_{20}\}$-type cluster found in $Na_{20}[Mo_{75}V_{20}O_{270}(H_2O)_{70}Na_{10}(SO_4)_{10}] \cdot$ ca. $150H_2O$: (a) $\{V_{20}Mo_{10}\}$ framework structure of the $\{Mo_{75}V_{20}\}$-type cluster with 30 vertices and 32 faces (20 triangles and 12 pentagons) spanned by 20 V^{IV} (red) and 10 Mo^{VI} (blue) centers emphasizing the ring-shaped band formed by 10 V_3^{IV} triangles (red). Additional details: (1) one of the $\{(Mo)Mo_5\}$ capping 10 pentagonal faces; (2) pentagonal under-occupied array built up by five of the MoO_6 octahedra capping the other two pentagonal faces (gray); and (3) one of the two encapsulated $\{NaSO_4\}_5$-type rings (Na positions: green, SO_4 tetrahedra: yellow). (b) Polyhedral representation of the (approximately) spherical structure of the complete $\{Mo_{75}V_{20}\}$-type cluster (for further details see Ref. [39]).

properties. For instance, a spin topology actively investigated at present in this respect is that of the so-called Kagomé lattice (Fig. 14a) [41].

As the physics of degenerate states is particularly sensitive to small perturbations, large variations in the properties exhibited by such systems may be expected. Typical examples, which illustrate this point, may be found in the extensive literature regarding the physics of Jahn–Teller systems, or in that regarding the properties of mixed-valence compounds [42].

In molecular magnetism, rings have been largely investigated in order to extrapolate the thermodynamic properties of infinite chains, and/or of larger rings [43,44]. In this respect, the V_{20} ring in $\{Mo_{75}V_{20}\}$ is a model for a chain (Fig. 14b), also indicating possible next-nearest neighbor interactions to be discussed now [45].

The most straightforward approach to calculate special thermodynamic properties of $\{Mo_{75}V_{20}\}$, and in particular its magnetic susceptibility, is that of calculating the energy levels of the spin hamiltonian:

$$\mathbf{H} = \sum_{i \neq j} J_{ij}\ \mathbf{S_i S_j}$$

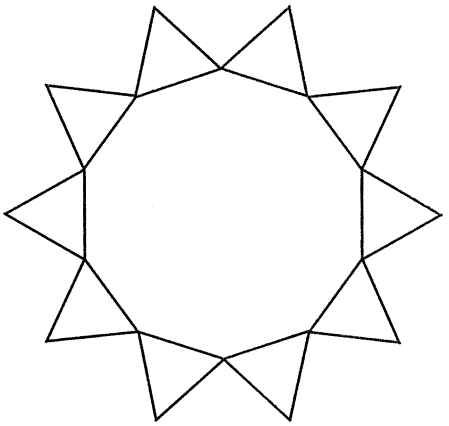

Fig. 13. Topology of the exchange pathways in the V_{20} ring of the $\{Mo_{75}V_{20}\}$ cluster. Only nearest neighbor interactions are considered.

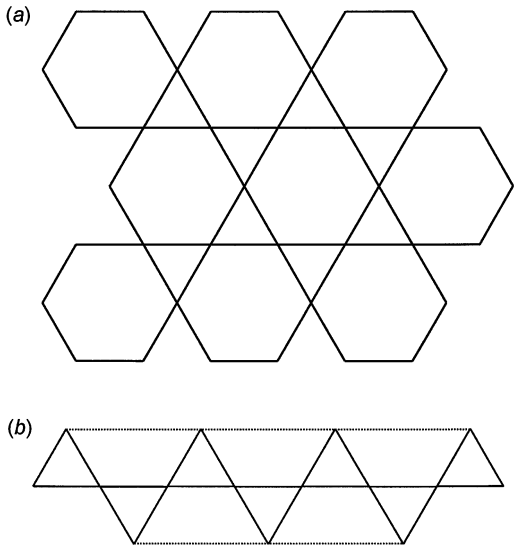

Fig. 14. (a) Scheme of a Kagomé lattice. (b) Topology of the exchange interactions in a chain equivalent to the V_{20} ring.

where the sum is over all spins of the ring, but the total number of states, $(2s+1)^{20} = 1\,048\,576$, is very high. This would—even using symmetry arguments in order to reduce the size of the matrices—require the diagonalization of matrices still too big to be handled (compare the corresponding term for the $\{Mo_{72}Fe_{30}\}$ cluster, 6^{30}, which is approximately equal to one third of Avogadro's number). It turned out that it is possible to describe the magnetic properties of the relevant

ten-membered ring by extrapolating calculations on smaller rings. The basis for this is the rapid convergence of the calculated magnetic susceptibility in antiferromagnetic rings, independent of the number of spins in the ring.

The procedure implies calculating χ for rings of increasing size. If the values are considered per vanadium ion, it is seen that at high temperatures the values calculated rapidly converge and become essentially identical to each other. Therefore, it may be reasonable to assume that the values remain approximately constant for the larger rings. Naturally, the treatment can be used down to the lowest temperature where the calculated values for different rings converge.

Calculations for rings consisting of 3–8 triangles (using a larger range of coupling constants for the smaller rings, but only a limited set of values for the larger rings) showed that the results for the $\{Mo_{75}V_{20}\}$ cluster are best described by referring to a ring of six triangles containing 12 spins (Fig. 15). Sample calculations with $J = 200\ cm^{-1}$ and J' varying between 0 and 150 cm^{-1} show that, for $J' = 0$, the limit value of χT at low temperature is 2.25 emu K mol^{-1}, in agreement with six uncoupled electrons (taking into account that the spins at the vertices of the triangles are uncorrelated to the other spins in case $J' = 0$). Therefore, the ring of triangles behaves like a six-membered ring, plus six uncorrelated spins. If the J' constant is allowed to differ from zero, χT goes to zero at increasingly higher temperatures corresponding to the fact that the ground state becomes a singlet, well separated from excited states except for a narrow range around $J' = 110\ cm^{-1}$, where the singlet and triplet states are almost degenerate as a consequence of spin frustration, and χT tends to the value expected for two uncorrelated spins $s = 1/2$.

The temperature dependence of χT for the $\{Mo_{75}V_{20}\}$ cluster is shown in Fig. 16. At room temperature, the value of ca. 5 emu K mol^{-1} is much smaller than expected for 20 uncoupled oxovanadium(IV) ions, 7.5 emu K mol^{-1}, indicating

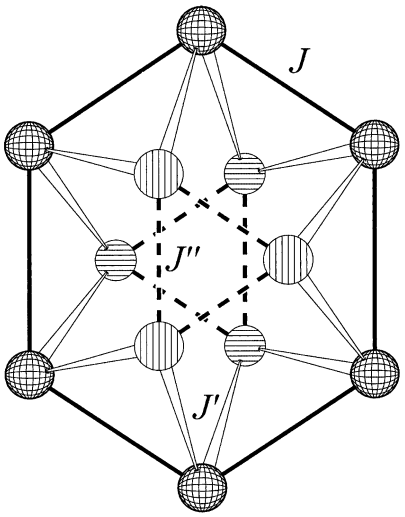

Fig. 15. Sketch of the exchange pathways in a ring of six triangles with three vertices pointing above and three below the main plane containing the six spins, showing the interaction pathways J, J', and J''.

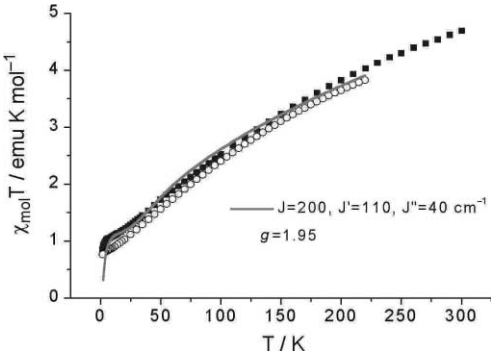

Fig. 16. Temperature dependence of $\chi_{mol}T$ of fresh (empty circles) and aged (filled squares) samples of the $\{Mo_{75}V_{20}\}$ compound. The solid gray line corresponds to the calculated value for a ring of six triangles, rescaled to 20 spins (see text).

that there is a significant antiferromagnetic coupling. The value of χT decreases smoothly with decreasing temperature and shows a hint of a plateau at ca. 0.8 emu K mol^{-1}.

The experimental values of χT at low temperature seem to level at the value of two uncorrelated $s = 1/2$ spins ($\chi T = 0.75$ emu K mol^{-1} for $g = 2.0$). Moreover, the magnetization vs. field curve recorded at 2.4 K is well reproduced by 2.1 times the value of the Brillouin function for $s = 1/2$. Despite the fact that the behavior at low temperature, typical of two uncorrelated $s = 1/2$, can be reproduced when $J'/J = 0.55$, such a model cannot reproduce the χT variation in a wide range of temperatures. Therefore, it was necessary to introduce a third exchange constant, connecting two vanadium ions at the vertices of the triangles that are on the same hemisphere around the six-membered ring (Fig. 15). This exchange interaction does not destroy the spin frustration as the vertices of the triangles form rings of odd numbers of spins. It is interesting to note that this particular behavior is different for rings consisting of $4n$ triangles. For these, the polygons connected through J'' have an even number of sites, and the ground state within the polygons is $S = 0$. Therefore, no plateaus are observed in this case. This behavior, again, is typical for spin frustration.

The experimental data can be satisfactorily fitted using the calculated curves for rings of six triangles and on rescaling the χT values from 12 to 20 vanadium centers (Fig. 16). It must be stressed here that the low temperature value in the case of frustration effects is expected to be two times the χT value for $s = 1/2$ for both the model cluster of 12 spins and the real cluster of 20 spins. The rescaling procedure of the calculated χT values which is therefore no longer valid for the low temperature limit, overestimates the low temperature χT (Fig. 16). The largest value for a coupling constant is needed for J, 200 cm^{-1}, and it correlates well with that previously reported for a similar compound, the $\{Mo_{57}V_6\}$ cluster [33]. Also the value of J', 110 cm^{-1}, compares well with that previously reported while J'', 40 cm^{-1}, is significantly larger than that previously observed for a similar bridge. But

its value should be considered only as an indication, possibly affected by the rescaling error mentioned above.

Minor differences in the low temperature behavior due to the aging of the samples can be justified with minor variations of the J parameters.

5. Outlook

The chemistry of the giant metal-oxide-based spherical species opens several new goals for chemistry and physics. Solid state chemistry may profit, in principle, from the opportunity to study nucleation processes involving rather large molecular spherical objects and to learn about basic principles of crystal growth and novel 'Aufbau' principles in solid state structures that involve connected fullerene-type cages. As the giant spheres can be functionalized in different ways, a completely new type of metal-oxide-based chemistry can be envisaged including a type of crystal engineering which allows cross-linking. Future aspects of this type of chemistry will be guided by the following key features of keplerate clusters:

1. The molecular structure and the size of keplerates can be controlled by variation of the linker groups.
2. Using larger linkers, holes open up that are accessible for small molecules.
3. Several keplerate spheres can be unlatched (resulting in basket-type clusters) and closed again thus enabling an exchange of the enclosed species [46].
4. High spin centers like $s = 5/2$ Fe^{III} can be used as linkers, with the possibility of generating novel spin topologies in nanomagnets.
5. Cross-linking of the cluster spheres extends the nanosized entities to a variety of network structures.
6. It is possible to generate novel supramolecular composites with magnetic keplerate-type shells and encapsulated electron reservoir nuclei (quantum-dots within magneto-dots) [47].
7. With surfactants composites can be generated which are soluble in organic solvents and can be used to generate monolayers and Langmuir–Blodgett films [48].
8. van der Waals clusters can be generated within the shell cavity while the formation of their structures can be directed [49].

Acknowledgements

We thank L. Cronin (Birmingham) for useful discussions and O. Delgado Friedrichs (Bielefeld) as well as D. Gatteschi and R. Sessoli (Florence) for their help in preparing this manuscript. We also thank the Deutsche Forschungsgemeinschaft and the Fonds der Chemischen Industrie for highly appreciated financial support.

References

[1] (a) A. Müller, P. Kögerler, C. Kuhlmann, Chem. Commun. (1999) 1347;
(b) A. Müller, F. Peters, M.T. Pope, D. Gatteschi, Chem. Rev. 98 (1998) 239;
(c) A. Müller, M.T. Pope (Eds.), Polyoxometalates: from Platonic Solids to Anti-Retroviral Activity, Kluwer, Dordrecht, 1994;;
(d) M.T. Pope, A. Müller, Angew. Chem. Int. Ed. Engl. 30 (1991) 34.
[2] A. Müller, P. Kögerler, H. Bögge, Struct. Bond. 96 (2000) 203.
[3] A. Müller, E. Krickemeyer, J. Meyer, H. Bögge, F. Peters, W. Plass, E. Diemann, S. Dillinger, F. Nonnenbruch, M. Randerath, C. Menke, Angew. Chem. Int. Ed. Engl. 34 (1995) 2122.
[4] (a) A. Müller, E. Krickemeyer, H. Bögge, M. Schmidtmann, C. Beugholt, P. Kögerler, C. Lu, Angew. Chem. Int. Ed. Engl. 37 (1998) 1220;
(b) C. Jiang, Y. Wei, Q. Liu, S. Zhang, M. Shao, Y. Tang, Chem. Commun. (1998) 1937.
[5] (a) A. Müller, J. Meyer, E. Krickemeyer, E. Diemann, Angew. Chem. Int. Ed. Engl. 35 (1996) 1206;
(b) A. Müller, C. Serain, Acc. Chem. Res. 33 (2000) 2.
[6] A. Müller, M. Koop, H. Bögge, M. Schmidtmann, C. Beugholt, Chem. Commun. (1998) 1501.
[7] (a) A. Müller, E. Krickemeyer, H. Bögge, M. Schmidtmann, C. Beugholt, S.K. Das, F. Peters, Chem. Eur. J. 5 (1999) 2114;
(b) A. Müller, E. Krickemeyer, H. Bögge, M. Schmidtmann, F. Peters, C. Menke, J. Meyer, Angew. Chem. Int. Ed. Engl. 36 (1997) 484.
[8] A. Müller, C. Beugholt, H. Bögge, M. Schmidtmann, Inorg. Chem. 39 (2000) 3112.
[9] L. Cronin, C. Beugholt, M. Schmidtmann, H. Bögge, E. Krickemeyer, P. Kögerler, A. Müller, Chem. Commun., submitted for publication.
[10] A. Müller, S.Q.N. Shah, H. Bögge, M. Schmidtmann, Nature 397 (1999) 48.
[11] (a) A. Müller, E. Krickemeyer, H. Bögge, M. Schmidtmann, F. Peters, Angew. Chem. Int. Ed. Engl. 37 (1998) 3360;
(b) A. Müller, V.P. Fedin, C. Kuhlmann, H. Bögge, M. Schmidtmann, Chem. Commun. (1999) 927.
[12] A. Müller, S. Sarkar, S.Q.N. Shah, H. Bögge, M. Schmidtmann, Sh. Sarkar, P. Kögerler, B. Hauptfleisch, A.X. Trautwein, V. Schünemann, Angew. Chem. Int. Ed. Engl. 38 (1999) 3238.
[13] A. Müller, S.Q.N. Shah, H. Bögge, M. Schmidtmann, P. Kögerler, B. Hauptfleisch, S. Leiding, K. Wittler, Angew. Chem. Int. Ed. Engl. 39 (2000) 1614.
[14] E. Haeckel, Kunstformen der Natur (1904), Prestel, München, 1998.
[15] (a) J. Kepler, Mysterium Cosmographicum, 1596;
(b) M. Kemp, Nature 393 (1998) 123.
[16] M. Goldberg, Tôhoku Math. J. 43 (1937) 104.
[17] D. Caspar, A. Klug, J. Quant. Biol. 27 (1962) 1.
[18] O. Delgado Friedrichs, A.W.M. Dress, A. Müller in:, M.T. Pope, A. Müller (Eds.), Polyoxometalates: Topology, Self-Assembly, Applications, Kluwer, Dordrecht, 2001.
[19] H.S.M. Coxeter, in: J.C. Butcher (Ed.), A Spectrum of Mathematics, Oxford University Press/ Auckland University Press, Oxford/Auckland, 1971.
[20] I. Stewart, Spiel, Satz und Sieg für die Mathematik, Birkhäuser, Basel, 1999.
[21] B. Listing, Gött. Studien 1 (1847) 811.
[22] P.W. Fowler, D.E. Manolopoulos, An Atlas of Fullerenes, Oxford University Press, Oxford, 1995.
[23] (a) O. Delgado Friedrichs, A.W.M. Dress, D.H. Huson, in: R. Corriu, P. Jutzi (Eds.), Tailor-Made Silicon–Oxygen Compounds: from Molecules to Materials, Vieweg, Braunschweig, 1996;
(b) O. Delgado Friedrichs, A.W.M. Dress, D.H. Huson, J. Klinowski, A.L. Mackay, Nature 400 (1999) 644;
(c) O. Delgado Friedrichs, A.W.M. Dress, A. Müller, M.T. Pope, Mol. Eng. 3 (1993) 9;
(d) A.W.M. Dress, in: L. Smith (Ed.), Algebraic Topology. In: Springer Lecture Notes in Mathematics, vol. 1172, Springer, Heidelberg, 1984;
(e) A.W.M. Dress, Adv. Math. 63 (1987) 196.
[24] P. Scott, Bull. London Math. Soc. 15 (1983) 401.
[25] A.W.M. Dress, D.H. Huson, Struct. Topol. 17 (1991) 5.

[26] (a) D. Gatteschi, L. Pardi, A.L. Barra, A. Müller, Mol. Eng. 3 (1993) 157;
(b) E. Coronado, C.J. Gomez-Garcia, Chem. Rev. 98 (1998) 273.
[27] (a) O. Kahn, Molecular Magnetism, Wiley, New York, 1993;
(b) R. Boca, Theoretical Foundations of Molecular Magnetism, Elsevier, Amsterdam, 1999.
[28] (a) R. Sessoli, D. Gatteschi, A. Caneschi, M.A. Novak, Nature 365 (1993) 141;
(b) J.R. Friedman, M.P. Sarachik, J. Tejada, R. Ziolo, Phys. Rev. Lett. 76 (1996) 3830;
(c) L. Thomas, F. Lionti, R. Ballou, D. Gatteschi, R. Sessoli, B. Barbara, Nature 383 (1996) 145;
(d) W. Wernsdorfer, R. Sessoli, Science 284 (1999) 133.
[29] G. Aromi, S.M.J. Aubin, M.A. Bolcar, G. Christou, H.J. Eppley, K. Folting, D.N. Hendrickson, J.C. Huffman, R.C. Squire, H.L. Tsai, S. Wang, M.W. Wemple, Polyhedron 17 (1998) 3005.
[30] (a) D. Gatteschi, L. Pardi, A.L. Barra, A. Müller, J. Döring, Nature 354 (1991) 463;
(b) A.L. Barra, D. Gatteschi, L. Pardi, A. Müller, J. Döring, J. Am. Chem. Soc. 114 (1992) 8509.
[31] D. Gatteschi, A. Caneschi, L. Pardi, R. Sessoli, Science 265 (1994) 1054.
[32] (a) A. Müller, E. Krickemeyer, S. Dillinger, H. Bögge, W. Plass, A. Proust, L. Dloczik, C. Menke, J. Meyer, R. Rohlfing, Z. Anorg. Allg. Chem. 620 (1994) 599;
(b) A. Müller, W. Plass, E. Krickemeyer, S. Dillinger, H. Bögge, A. Armatage, A. Proust, C. Beugholt, U. Bergmann, Angew. Chem. Int. Ed. Engl. 33 (1994) 849;
(c) A. Müller, J. Meyer, E. Krickemeyer, C. Beugholt, H. Bögge, F. Peters, M. Schmidtmann, P. Kögerler, M.J. Koop, Chem. Eur. J. 4 (1998) 1000.
[33] (a) A. Müller, W. Plass, E. Krickemeyer, R. Sessoli, D. Gatteschi, J. Meyer, H. Bögge, M. Kröckel, A.X. Trautwein, Inorg. Chim. Acta 271 (1998) 9;
(b) D. Gatteschi, R. Sessoli, W. Plass, A. Müller, E. Krickemeyer, J. Meyer, D. Sölter, P. Adler, Inorg. Chem. 35 (1996) 1926.
[34] A. Müller, M. Luban, C. Schröder, R. Modler, P. Kögerler, M. Axenovich, J. Schnack, P. Canfield, S. Bud'ko, N. Harrison, Chem. Phys. Chem. 2 (2001) 517.
[35] M. Axenovich, M. Luban, Phys. Rev. B 63 (2001) 100407.
[36] M. Luban, J. Schnack, R. Modler, Europhys. Lett., in press.
[37] A. Müller, E. Krickemeyer, S.K. Das, P. Kögerler, S. Sarkar, H. Bögge, M. Schmidtmann, Sh. Sarkar, Angew. Chem. Int. Ed. Engl. 39 (2000) 1612.
[38] (a) K.S. Murray, Coord. Chem. Rev. 12 (1974) 1;
(b) D.M. Kurtz, Chem. Rev. 90 (1990) 585;
(c) H. Weihe, H.U. Güdel, J. Am. Chem. Soc. 119 (1997) 6539.
[39] A. Müller, M. Koop, H. Bögge, M. Schmidtmann, F. Peters, P. Kögerler, Chem. Commun. (1999) 1885.
[40] J. Vannimenous, G. Toulouse, J. Phys. C 10 (1977) 537.
[41] K. Awaga, N. Wada, in: O. Kahn (Ed.), Magnetism: a Supramolecular Function. In: NATO ASI Series C, vol. 484, Kluwer, Dordrecht, 1996.
[42] K. Prassides (Ed.), Mixed Valency Systems: Applications in Chemistry, Physics, and Biology. In: NATO ASI Series C, vol. 343, Kluwer, Dordrecht, 1991.
[43] K. Bärwinkel, H.-J. Schmidt, J. Schnack, J. Magn. Magn. Mater. 220 (2000) 227.
[44] J. Schnack, Phys. Rev. B 62 (2000) 14855.
[45] D. Gatteschi, R. Sessoli, A. Müller, P. Kögerler, in: M.T. Pope, A. Müller (Eds.), Polyoxometalates: Topology, Self-Assembly, Applications, Kluwer, Dordrecht, 2001.
[46] A. Müller, S. Polarz, S.K. Das, E. Krickemeyer, H. Bögge, M. Schmidtmann, B. Hauptfleisch, Angew. Chem. Int. Ed. Engl. 38 (1999) 3241.
[47] A. Müller, S.K. Das, P. Kögerler, H. Bögge, M. Schmidtmann, A.X. Trautwein, V. Schünemann, E. Krickemeyer, W. Preetz, Angew. Chem. Int. Ed. Engl. 39 (2000) 3414.
[48] D. Volkmer, A. Du Chesne, D.G. Kurth, H. Schnablegger, P. Lehmann, M.J. Koop, A. Müller, J. Am. Chem. Soc. 122 (2000) 1995.
[49] A. Müller, V.P. Fedin, C. Kuhlmann, H. Bögge, M. Schmidtmann, Chem. Commun. (1999) 927.